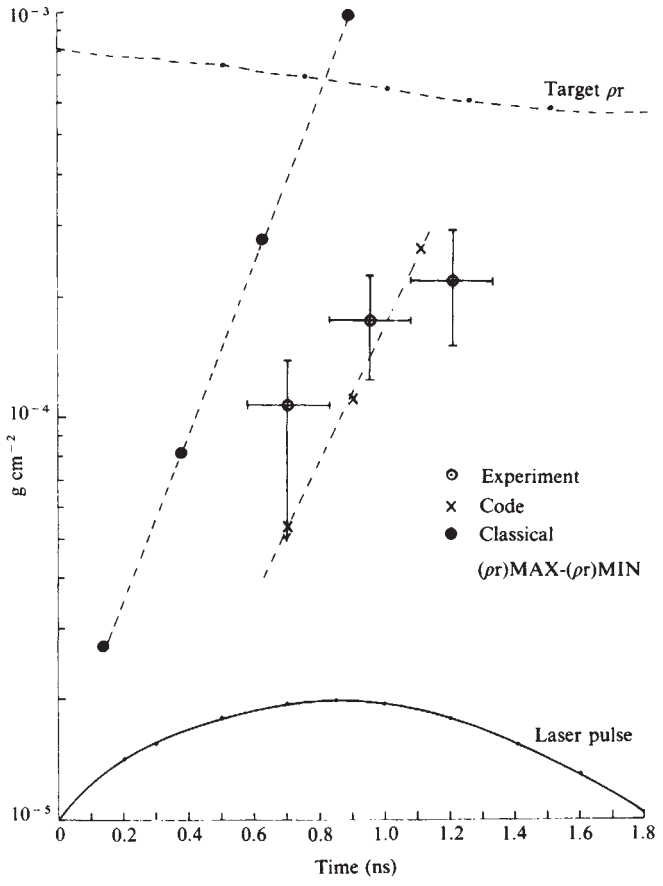

Fig. 3 Graph of modulation in target areal density from the three experimental measurements in Fig. 2*c*. Also shown are the results of two-dimensional fluid simulations and the modulation expected of a classically growing instability.

of 10 Å (in I_A), with a rapid fall at shorter wavelength. The variation of the X-ray intensity reaching the streak camera with Al target thickness was calculated from the spectrum and the transmission of the filters, giving agreement with the 55% transmission observed through a 3-μm Al foil in a separate experiment.

An X-ray streak photograph of the transmission of such an accelerated target is shown in Fig. 2, with the corrugation parallel to the direction of streaking. Initially there is, as expected, no variation of transmission across the target, but as the instability grows, mass is redistributed and modulations in the transmission with a period of 20 μm can be seen. In control experiments with no initial corrugation, no such regular modulation is observed.

The film density modulations evident in Fig. 2 were converted to mass per unit area modulation by using the calculated variation of spectrally integrated transmission with Al thickness as described above. The amplitude of the modulation is shown in Fig. 3 as a function of time, the errors representing the spread in the amplitude of the eight modulations evident at late time in Fig. 2.

The average growth rate from Fig. 3 is $1.6 \pm 0.5 \times 10^9\ s^{-1}$, with some evidence of saturation. Figure 3 also shows the classical growth, taken from $(ka)^{1/2}$ and the acceleration scaled from the measurements shown in Fig. 1. The classical growth is started, in Fig. 3, at the onset of target motion with an initial amplitude determined by projecting back the slope of the experimental observations to zero time. The initial surface perturbation is not an R–T eigenmode, as there is no initial velocity perturbation, and this can cause some delay in the growth of an R–T mode[8]. However, it can be seen that the observed growth rate is $\sim 0.3 \times (ka)^{1/2}$.

The experiment has been simulated using a two-dimensional Eulerian fluid code[9]. An absorbed irradiance of $2.0 \times 10^{13}\ W\ cm^{-2}$ was used so that the distance moved by the foil in the simulation matched the observed motion. A corrugated target as used in the experiment seeded the growth of an instability at the desired wavelength. The code predictions of growth in mass–density modulations (after convolving with a pinhole response) are also shown in Fig. 3.

The experimental measurements of Fig. 3 are lower than both the classical value and the simulated value. This is not due to ablating too much material from the target: the initial areal density is $0.8\ mg\ cm^{-2}$ and the decrease due to ablation[7] is shown in Fig. 3. The analysis of the Al transmission assumes the cold X-ray mass attenuation coefficients. However, the code values for the temperature and a local thermodynamic equilibrium ionization equation shows that this produces a negligible error. However, several phenomena are omitted or modelled inaccurately in the simulation, including radiation transport, equation of state, ion viscosity and magnetic field generation.

In conclusion, observations of the growth of area density modulations at a rate of $0.3 \times (ka)^{1/2}$ have been observed. Although these results are incomplete, in that data have so far only been obtained for one k value, it is nevertheless encouraging for laser-driven compression that the growth rate is so low, significantly less than classical, as has been predicted by numerical simulation[5].

We acknowledge helpful conversation with W. C. Mead. A.J.C. was supported by a SERC studentship.

Received 13 May; accepted 14 July 1982.

1. Lord Rayleigh, *Theory of Sound* 2nd edn, Vol. 2 (Dover, New York, 1945).
2. Taylor, G. I. *Proc. R. Soc.* **A201,** 192 (1930).
3. Nuckolls, J. H., Wood, L., Thiessen, A. & Zimmerman, G. *Nature* **239,** 139 (1972).
4. McCrory, R. L., Monteith, L., Morse, R. L. & Verdon, C. P. *Phys. Rev. Lett.* **46,** 336 (1981).
5. Emery, M. H., Gardner, J. H. & Boris, J. P. *Phys. Rev. Lett.* **48,** 677 (1982).
6. Ross, I. *et al. IEEE J. Quant. Elect.* **QE17,** 1653 (1981).
7. Goldsack, T. J. *et al. Opt. Commun.* **42,** 55 (1982).
8. Lindl, J. D. & Mead, W. C. *Phys. Rev. Lett.* **34,** 1273 (1975).
9. Pert, G. *J. comp. Phys.* **43,** 111 (1981).

Density-driven interstitial water motion in sediments

D. L. Musgrave & W. S. Reeburgh

Institute of Marine Science, University of Alaska, Fairbanks, Alaska 99701, USA

Sediment depth distributions and fluxes of dissolved chemical substances have been interpreted as being a result of reaction, diffusion, bioturbation and irrigation[1,2]. However, several studies suggest that density-driven convection[3] can alter the depth distribution and increase the fluxes of dissolved substances when density decreases below the sediment surface[4–7]. We present here temperature–time series measurements for a freshwater lake undergoing autumn cooling. These are the first *in situ* observations of heat transport due to motion of interstitial waters over periods of less than 1 hour. Density, calculated from temperature, decreases with depth at the time and place that this motion occurs.

Temperature was measured by inserting a multi-thermistor plastic probe into the sediments. The probe was made of 2.5-cm PVC pipe with glass bead thermistors mounted along its length. The thermistors were pushed through drilled 2-nm diameter holes until the sensing element protruded at least 1 nm beyond the exterior wall of the pipe. Electrical leads from each thermistor were fed through the interior of the pipe to resistance bridges at the top of the probe. The probe was filled with polyurethane foam to reduce its thermal mass. Self-heating of the thermistors was negligible. Time response of the probe to temperature changes was < 30 s. The voltage output from each thermistor was recorded on magnetic tape at 5-min intervals with a 12-bit Datel DL-2 data logger. All thermistors were corrected for

0028-0836/82/380331—04$01.00

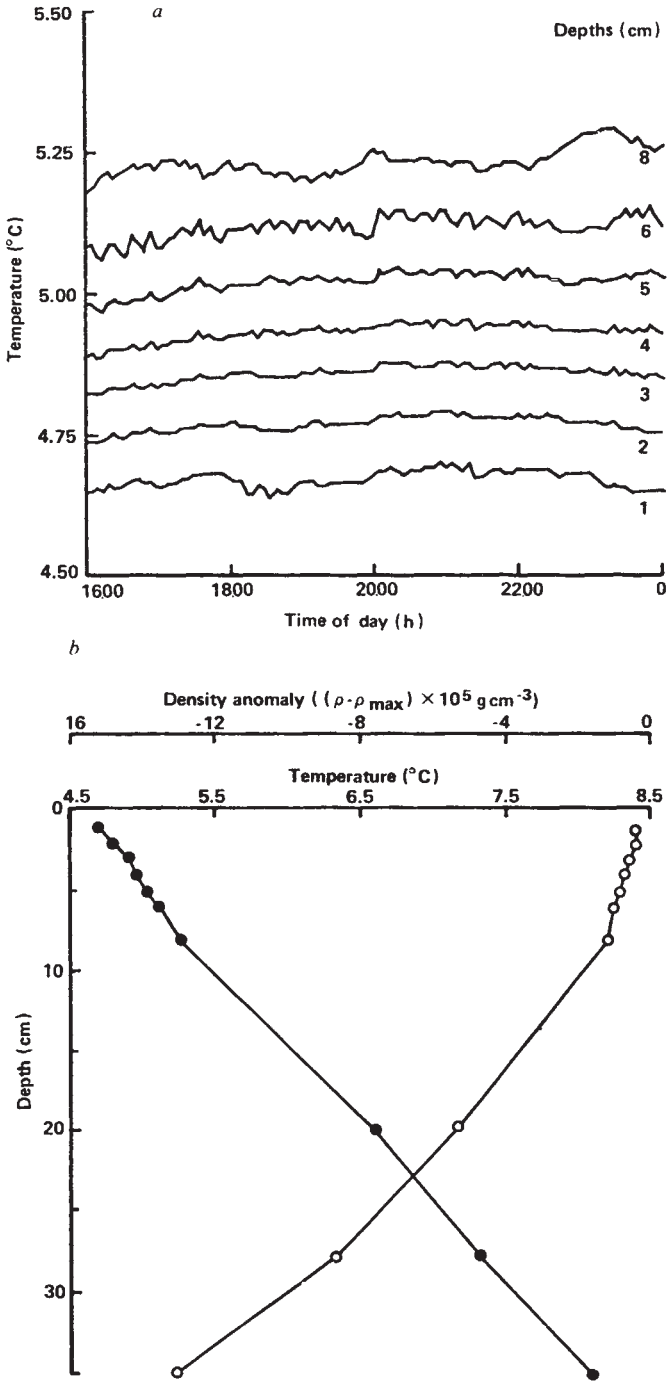

Fig. 1 *a*, Temperature records at depths below the sediment surface (27 October 1979; 0.75 m water depth). The record at 20 cm showed no temperature fluctuations. *b*, Temperature (●) and density (○) profiles in sediments (27 October 2000 CST). Density was calculated from temperature[9].

gain and supply voltage changes by monitoring a reference voltage and the bridge supply voltage. The probes were calibrated at 2 °C intervals between 0 and 20 °C in a temperature bath controlled to 0.001 °C (Northwest Regional Calibration Centre). Although the probes were not recalibrated immediately after deployment, comparisons between calibrations indicated long-term (6-month) accuracy for each thermistor bridge of 0.01 °C. Short-term (1-day) stability is determined by the resolution of the data logger (1 bit in 12 over 27 ° = 0.007 °C), so changes in temperature can be resolved to this limit. The *in situ* temperature distributions were disturbed by the initial insertion of the probe for 4 hours. All temperatures reported here were from periods several days after the probe insertion.

We placed three probes in the sediments of Lake 227 of the Experimental Lakes Area, Ontario, Canada, at water depths of 0.75, 1.25, and 1.75 m. These sediments have high, nearly constant porosity (0.85) and organic content (48% dry weight measured by loss of weight on ignition at 900 °C)[4,8]. The particle size data for two similar, nearby lakes at ELA show the following distribution[8]: sand (>50 μm) 13%; silt (2–50 μm) 75%; clay (<2 μm) 12%. The probes were in place from mid- to late-October 1979, in anticipation of bottom-water density increases due to autumn cooling. The diurnal temperature range at the sediment surface of Lake 227 was <1 °C. The temperature increased with depth into the sediments (Fig. 1*b*). Temperatures varied smoothly at all depths until 25 October. At this time the temperatures in the upper 8 cm of the sediments at 0.75 and 1.25 m water depth developed transient perturbations that were independent of temperature variations at the sediment surface (Fig. 1*a*). The perturbations continued (with maximum amplitudes of 0.06 °C at depths of 6 and 8 cm) until the probes were retrieved.

The observed temperature fluctuations are probably caused by interstitial water motion due to buoyancy forces. However, they may be caused by other mechanisms, namely: (1) noise generated by the data acquisition system; (2) interstitial water motion caused by biological processes such as bioturbation and irrigation; and (3) interstitital water motion due to physical forces other than buoyancy.

We rely on our own calibration data and the long-term behaviour of the data acquisition system (as indicated by the temperature–time series) to address questions of noise due to instabilities of the acquisition system. Any noise-like error due to electronic instabilities of the data logger should appear in all channels because all input signals are processed in serial mode and thus employ the same circuitry. Visual inspection of the time series shows that the temperature fluctuations occur simultaneously only over a few adjacent thermistors. The relative stability of thermistors at other depths indicates that the electronics were introducing no sources of noise (and that the probe was not being physically moved in to or out of the sediment). There are two facts that indicate that the fluctuations are not caused by failure of electronics outside of the data logger: (1) before 25 October, fluctuations in the frequency range of the observed fluctuations do not occur in any channel; (2) the fluctuations in adjacent thermistors are coherent. Therefore, we are quite confident that we are observing *in situ* temperature fluctuations.

The possibility that the fluctuations are caused by bulk sediment redistribution or irrigation by infauna is not consistent with this environment. Hesslein[4] showed that the solid phase of these sediments has not been redistributed after deposition. Infauna, if present, would disturb the sediment solid phase and therefore we take Hesslein's remarks as evidence that no infauna exist in these sediments. The absence of temperature fluctuations before 25 October corroborates this conclusion. We rule out the possibility of bubble ebullition for the same reasons.

Physical mechanisms that could cause interstitial water motion include ground water seepage, surface wave phenomena and buoyancy. Ground water flow is negligible, which is consistent with absence of the fluctuations for long intervals of time. In any case, we do not expect fluctuations of ground water flow with the regularity or high frequency of the observed fluctuations. Forced convection in the sediments due to surface waves or seiches is precluded by the lack of coherent temperature fluctuations in the upper sediments and concomitant attenuation of the surface fluctuations with depth in sediments.

The temperature gradient is destabilizing below the sediment surface due to autumn cooling of the bottom waters (Fig. 1) and may cause density-driven convection, leading to the observed temperature fluctuations. Quay[10] shows that dissolved solids can significantly affect water density in Lake 227. The main effect in this context would be an offset in the density

since all solute gradients are above depths of 10 cm. The density gradients would not be affected.

The possibility of density-driven (free) convection leads us to consider the Rayleigh number[3], Ra, defined by

$$Ra = \frac{\alpha \Delta T K (\rho c)_f H}{\lambda_B}$$

where K is the hydraulic conductivity, α is the thermal expansion coefficient, $(\rho c)_f$ is the heat capacity of the interstitial water, λ_B is the bulk thermal conductivity coefficient of the saturated porous medium, and H and ΔT are the scale depth and temperature difference, respectively. This dimensionless number is a measure of the ratio of the destablizing buoyancy force to the stabilizing process of diffusion. According to theory and laboratory experiments, the thermal Rayleigh value must exceed a critical value ($Ra_c = 40$) before the motions induced by small horizontal temperature perturbations can maintain free convection. This critical value is derived assuming a saturated, homogenous, porous medium of depth H bounded above and below by impermeable, isothermal plates across which a destabilizing temperature difference, ΔT, is imposed. The equation of state relating density to temperature is linear and the system is assumed to be time independent. Nonlinear density–temperature relationships[11], periodic boundary conditions[12], nonhomogeneous[13] or anisotropic porous medium[14] or permeable boundaries[15] can all act to reduce the critical Rayleigh number, although probably not by a factor of 10. Therefore, we take the value of 40 as an order of magnitude estimate for the critical Rayleigh number.

The Rayleigh number was estimated using the following assumptions. The high porosity permits the use of the thermal diffusivity, κ, of water (1×10^{-3} cm^2 s^{-1}) for the quotient $\lambda_B/(\rho c)_f$. Our efforts at measuring *in situ* hydraulic conductivity failed in Lake 227 so we estimated it to be 10^{-1} cm, which is similar to the value for sands. This is a high value but we think it is justified by the flocculent nature of Lake 227 sediments. The amplitude of the annual temperature cycle at the 1 m water depth is 20 °C which we take for ΔT and the sediment depth, H, is 10 m. Using these values the maximum value of the Rayleigh number is 200, which is realized only when the amplitude of the annual temperature cycle is realized across the whole depth of the sediments. When this happens the interstitial water is freely convecting.

However, there is a period of time after autumn cooling begins when ΔT is not realized over the whole sediment depth. In transient systems, a time-dependent Rayleigh number can be calculated based on the product $H\Delta T$ where H and ΔT are scaled according to diffusion theory and both change with time. When this time-dependent Rayleigh number first exceeds the critical value at time t_c convection ensues over the depth $H(t_c)$ (ref. 16). The convecting layer erodes the stable layer below and H increases faster than purely diffusive transport would allow until the convecting layer reaches the sediment basement and ΔT is realized across the entire sediment depth.

Since we do not have temperatures below 35 cm we estimate H and ΔT as a function of time as follows. The temperature of the bottom water in contact with the sediments at 1 to 2 m water depth was 22 °C from 1 June to 1 September. For this time interval we calculate the diffusive scale length to be 200 cm, which is the depth to which summer heating occurs. We assume that on 1 September the sediments to 200 cm are at 22 °C, and the sediment surface begins cooling linearly with time to the observed temperature of 4.4 °C on 30 October. The temperature–depth distribution as a function of time, for a system undergoing surface cooling at a linear rate, is given by Carslaw and Jaeger[17]. If we define the scale depth, H, as the depth at which the temperature is 0.0567 times the temperature difference between the temperature much deeper in the sediment and the temperature at the surface, then H is given by $H = 2\sqrt{\kappa t}$ where t is the time after 1 September. The scale temperature difference, ΔT, is then given by $\Delta T = mt\,(0.0567 - 1)$, where m is the rate of cooling. The product $H\Delta T$ increases as the 3/2 power of time and on 28 October is estimated to be 2×10^3 °C cm.

The Rayleigh number on this date is 20 and certainly within the range of the critical value, considering that this estimate is valid over an order of magnitude. The appearance of the temperature fluctuations at this time indicates that the estimate is fairly good.

Although we think the temperature fluctuations are due to free convection, they are not characteristic of linear, steady-state, convection. Horne and O'Sullivan[18] have shown that oscillatory convection occurs at Rayleigh numbers above 240. Our estimate of the Rayleigh number is lower by 10 times, although we think that it could be an underestimate. However, the absence of temperature fluctuations below 15 cm is not consistent with the oscillatory systems described by Horne and O'Sullivan.

The density calculated from temperature shows negligible gradients in the upper few centimetres due to the density extremum at 4 °C. So at the time the fluctuations occur, the unstable convecting layer is bounded above by a stable quiescent layer. Free fluids near the density extremum at 4 °C show large temperature fluctuations at the boundary between the stable and convecting layers[19]. These fluctuations have been interpreted as internal waves propagating along the interface[20]. The dynamics of flow in porous media do not allow inertial effects, and phenomena such as internal waves do not exist. However, we think that the convecting layer, beneath a shallow stable layer, causes the observed fluctuations in some manner whose details have been examined theoretically.

The increase in heat transport due to convection is quantified by the Nusselt number which is the ratio of heat flux across a convecting layer to the heat flux across the same layer assuming purely diffusive transport. The Nusselt number does not strictly apply to transient convection but we can get an order of magnitude of the increased transport from theoretical and experimental studies which give the Nusselt number as a function of the Rayleigh number[3]. Near the critical Rayleigh number the Nusselt number is just greater than 1. In Lake 227 the Rayleigh number continues to grow with time until the convecting layer intersects the impermeable rock below the sediments at 10 m. The Rayleigh number based on this depth is 200 and the maximum Nusselt number is then 4. The increase in transport of solutes cannot be readily estimated. In systems that are undergoing circular motion, there is no net water transport across any horizontal surface and net transport of solutes occurs only if vertical gradients in concentration exist. This implies that the increase in solute transport will also depend on the strength of the solute sink (or source) in the sediments. We know of no theory to describe the increase in transport of a passive solute as a function of the Rayleigh number and sink strength. We only mention that solute diffusivities are typically 10^{-2}–10^{-3} times the thermal diffusivity and therefore seem more susceptible than heat to increased transport by convection.

This work was supported by NSF grants OCE 78-20896, OCE 80-26046 and a Jessie Smith Noyes Foundation Fellowship to D.L.M. We thank R. H. Hesslein and D. W. Schindler for their assistance, and W. D. Harrison for helpful discussions. Contribution no. 489 from the Institute of Marine Science, University of Alaska.

Received 21 December 1981; accepted 9 July 1982.

1. Berner, R. A. *Principles of Chemical Sedimentology* (Princeton University Press, 1971).
2. Berner, R. S. *Early Diagenesis. A Theoretical Approach* (Princeton University Press, 1980).
3. Combarnous, M. A. & Bories, S. A. *Adv. Hydrosci.* **10**, 232–309 (1974).
4. Hesslein, R. H. *Can. J. Fish. aquat. Sci.* **37**, 545–551 (1980).
5. Thorstensen, D. C. & Mackenzie, F. T. *Geochim. cosmochim. Acta* **28**, 1–19 (1974).
6. Harrison, W. D. & Osterkamp, T. E. *J. geophys. Res.* **83**, 4707–4712 (1978).
7. Smetacek, V. F., von Bedungen, F., von Brockel, K. & Zeitzschel, B. *Mar. Biol.* **34**, 373–378 (1976).
8. Brunskill, G. J., Povoledo, D., Graham, B. W. & Stainton, M. P. *J. Fish. Res. Bd Can.* **28**, 277–294 (1971).
9. Kell, G. S. *J. Chem. Engng Data* **12**, 66–69 (1967).
10. Quay, P. D. thesis, Columbia Univ. (1977).
11. Ray-shing Wu, Cheng, K. C., & Craggs, A. *Numerical Heat Transfer* **2**, 303–318 (1979).
12. Chhuon, B. & Caltigorone, J. P. *J. Heat Transfer* **101**, 244–248 (1979).
13. Green, T. & Freehill, R. L. *J. appl. Phys.* **40**, 1759–1762 (1969).

14. Wooding, R. A. *Proc. 2nd Workshop Geotherm Reservoir Engng*, 339–345 (Stanford University Press, 1976).
15. Nield, D. A. *Wat. Resour. Res.* **4**, 553–560 (1968).
16. Elder, J. W. *J. Fluid Mech.* **32**, 69–96 (1968).
17. Carslaw, H. S. & Jaeger, J. C. *Conduction of Heat in Solids* 2nd edn (Oxford University Press, 1959).
18. Horne, R. N. & O'Sullivan, M. J. *J. Fluid Mech.* **66**, 339–352 (1974).
19. Townsend, A. A. *Q. Jl R. met. Soc.* **90**, 248–259 (1964).
20. Townsend, A. A., *J. Fluid Mech.* **24**, 307–319 (1966).

Thermal expansion effects in deep-sea sediments

T. J. G. Francis

Institute of Oceanographic Sciences, Brook Road, Wormley, Godalming, Surrey GU8 5UB, UK

Understanding how *in situ* heating affects unlithified deep-sea sediments is important for both geological and practical reasons. Deep-sea drilling by *Glomar Challenger* over the past decade has revealed several places where magma has intruded sediment to form sills and the heat released by a large sheet of molten rock has been shown to produce substantial changes on the sediments in its vicinity[1]. Another example is the burial of hot canisters of high-level radioactive waste within the sediments of the ocean floor, which has been proposed as a solution to the problem of disposing of this material[2]. I consider here the physical effects which high temperatures might produce in deep-sea sediments. Substantial chemical effects are also likely, but these are not discussed. In practice, the physical and chemical effects would work together in modifying the original sediment.

The individual thermal behaviour of the components of a sediment is straightforward and well understood. The pressure–volume–temperature relations for seawater differ very little from those for pure water[3]. The specific volume of pure water as a function of temperature and pressure has been tabulated by Burnham *et al.*[4] and can be corrected with the work of Saunders[5] to give values for seawater. The resulting thermal expansion of seawater at pressures of 200 and 500 bar is shown in Fig. 1. It is clear that the volume thermal expansion coefficient, defined as $1/V(\partial V/\partial T)_P$ is not constant but increases with increasing temperature. In contrast, the thermal expansion of most rock-forming minerals can be adequately described by a constant coefficient in the temperature range 0–400 °C (ref. 6). The thermal expansion of one particular solid material, quartz, is also shown in Fig. 1 to illustrate the contrast in thermal expansivity between the solid and liquid components of the sediment. One can conclude that the thermal expansivity

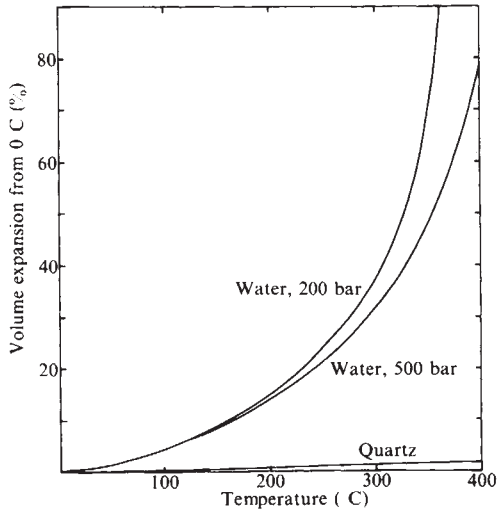

Fig. 1 The thermal expansion of water/seawater at 200 and 500 bar. The expansion of quartz, measured at atmospheric pressure, is shown for comparison. As a general rule the thermal expansivity of sedimentary pore water is two orders of magnitude greater than that of the solid component.

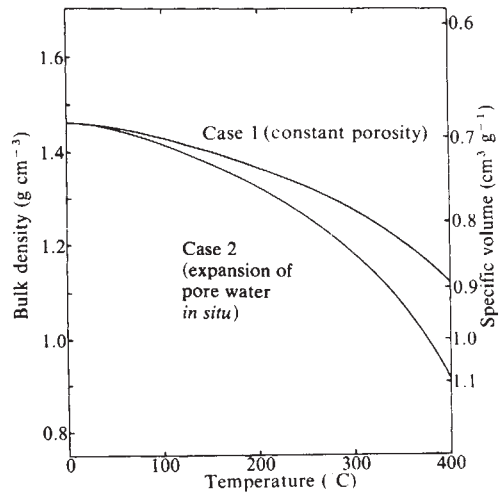

Fig. 2 The effect of thermal expansion on the density of a sediment at an ambient pressure of 500 bar. Initial porosity of sediment 0.75; grain density 2.7 g cm^{-3}.

of sedimentary pore water is some two orders of magnitude greater than that of the solid component. For the present purposes, the expansion of the solid component of the sediment is regarded as negligible.

The manner in which a sediment expands will be affected by the way in which heat is applied. The heating of sediment *in situ* is unlikely to be a uniform process. With magma intrusion and the burial of radioactive waste strong temperature gradients are likely to exist, both during the development of the temperature field and in the steady state. Two limiting cases to the way in which a sediment responds to heating can be considered. The first is the fully drained case, where the sediment matrix remains unchanged and expanding pore water is accommodated by flowing away from the source of heat. The porosity of the sediment is unchanged, but the bulk density of the heated sediment is reduced because of the reduced density of the pore water. The bulk density ρ is related to the solid particle density ρ_s and the fluid density ρ_f by $\rho = (1-\phi)\rho_s + \phi\rho_f$ where ϕ is the fractional porosity. This expression can be used to calculate the density of the heated sediment since ρ_f is known as a function of temperature and ρ_s and ϕ are unchanged (case 1, Fig. 2). The second limiting case is where the pore water remains in place as it expands, disrupting the sedimentary matrix in the process. The bulk density of the heated sediment will be reduced both because of its increased porosity and because the density of the pore water is reduced. If a volume of sediment V weighs W and the weights of the solid and fluid components are W_s and W_f respectively, then

$$V = \frac{W_s}{\rho_s} + \frac{W_f}{\rho_f} = \frac{W}{\rho}$$

where in the undrained case W, W_s, W_f and ρ_s are constants. For a sediment of initial porosity 0.75 and grain density 2.7 g cm^{-3}, the expression becomes

$$\rho = \frac{1.4633}{0.25 + (0.7883)/(\rho_f)}$$

Values obtained from this equation corresponding to an ambient pressure of 500 bar are shown as case 2 in Fig. 2.

The behaviour of a sediment in reality will fall between these two limiting cases. One would expect a highly permeable sand to behave in a fully drained manner (case 1). A uniformly heated, impermeable clay might tend to follow case 2. As already mentioned, however, uniform heating is unlikely and strong temperature gradients are probable. In the second case, these would give rise to pore pressure gradients, pore water flow would occur to relieve the pressure and collapse of the expanded sediment matrix back towards its original porosity would result. Pore water flow will be facilitated by the increase

0028–0836/82/380334—03$01.00